# Swelling and Elastic Properties of Polyelectrolyte Gels

**R. Skouri, F. Schosseler, J. P. Munch, and S. J. Candau***

*Laboratoire d'Ultrasons et de Dynamique des Fluides Complexes, URA 851, Université Louis Pasteur, 4 rue Blaise Pascal, 67070 Strasbourg Cedex, France*

*Received July 22, 1994; Revised Manuscript Received September 26, 1994®*

ABSTRACT: Ionized poly(acrylic acid) gels were studied both at concentrations close to the concentration of preparation and at swelling equilibrium. In the first experimental condition, the introduction of electrostatic interactions decreases the shear modulus. The addition of salt screens these interactions and allows one to recover the shear modulus of unneutralized gels. The correlation of these effects with light scattering results suggests that they are related to a change of the gel microstructure with electrostatic interactions. The swelling equilibrium of these gels if found to scale like the ratio of the ionization degree to the Debye–Hückel screening parameter with an exponent 6/5. The shear modulus at swelling equilibrium is given by the simple affine deformation law for not too high swelling degrees (<200). For larger swelling ratios, the shear modulus increases with swelling ratio due to deviations from Gaussian elasticity. These results can be partly explained by a recently proposed model. Finally, the cooperative diffusion coefficient can be measured by kinetics of swelling experiments and its behavior does not follow the predictions of the same model, possibly due to the coupling of cooperative diffusion with the establishment of a Donnan equilibrium.

## Introduction

Electrostatic interactions modify deeply the behavior of polymeric gels. One of the most striking properties of polyelectrolyte gels is their ability to swell: some covalently cross-linked gels exhibit a swelling degree in water as high as 1000, which can be monitored by changing the ionic strength. This property is at the origin of the applications of these gels as superabsorbents.

From a more fundamental point of view, the understanding of the structure and the dynamics of charged gels remains a challenging problem. The complex behavior of polyelectrolyte systems is due mainly to both the long-range character of the Coulomb interactions and the effect of the counterions that ensure the electroneutrality.

The swelling behavior of charged gels has been described in the seminal work by Katchalsky et al.[1,2] and Flory and Rehner[3] as resulting from a balance between the elastic energy of the network and the osmotic pressure of the ions. In salt-free gels this osmotic pressure is due to the counterions that are confined inside the volume of the gel in contact with a water reservoir. In the presence of salt the osmotic pressure is associated with the establishment of a Donnan equilibrium. Katchalsky et al. considered also the effect of electrostatic interactions of the fixed charges on polymer chains.[1,2] As for the elastic free energy, the Flory expression derived from a Gaussian statistics of the chains was assumed.

These approaches are generally considered as the basic models to interpret the thermodynamic properties of polymeric gels. However, the comparison between experimental results and theoretical predictions is not always convincing, and several modifications to these basic models were proposed. These modifications dealt mainly with the osmotic pressure arising from the polymer–solvent interactions and with the effect of finite chain extension on the elasticity of the polymer network.[4–8] Full expressions for the free energy of the gels involve many parameters, and their use to fit the experimental data does not generally provide a physical picture of the gel.

Recently, a simple model for scattering properties of polyelectrolyte gels at swelling equilibrium was proposed by Barrat et al.[9] The model assumes that, in the weak screening limit where the Debye–Hückel screening length, $\kappa^{-1}$, is larger than the mesh size of the network, the swelling is driven by the osmotic pressure of the counterions. The tension created by this pressure is transmitted through the cross-links to the elastic chains, which behave as isolated chains with an applied force at their end points. Such a model predicts a simple scaling behavior of the equilibrium swelling degree as a function of the ionization degree $\alpha$. In the strong screening limit, in the presence of an excess of salt, the gels are expected to behave as neutral gels with an effective excluded volume controlled by the ratio $\alpha/\kappa$. This leads also to a simple scaling behavior of the equilibrium swelling degree with that parameter, which turns out to be the same as in the weak screening regime.

In this paper we report an experimental study on moderately cross-linked poly(acrylic acid) (PAA) gels prepared in the acid form and then neutralized to the desired degree of ionization. The aim of this study was to check whether the thermodynamic properties of these gels could be described by the simple approach quoted above.

The elastic properties of these gels were first examined at a polymer concentration close to that of preparation. The results show an intriguing behavior, namely, a decrease of the shear modulus upon increasing the ionization degree, and are discussed in terms of the mesoscopic structure of the gels, which can be probed by light scattering experiments.

In a second stage the gels were studied at swelling equilibrium. More specifically, we measured the swelling equilibrium degree, the shear modulus, and the diffusion coefficient, the latter being obtained from kinetics of swelling experiments. In the discussion we compare the results obtained at the concentration of preparation and at swelling equilibrium with the predictions of recently proposed models.[9–11]

® Abstract published in *Advance ACS Abstracts,* November 15, 1994.

0024-9297/95/2228-0197$09.00/0 

## Experimental Section

**A. Sample Preparation.** Sample preparation followed the procedure described in preceding papers.[12-14] Gels are prepared by radical copolymerization in an aqueous solution of acrylic acid and *N,N'*-methylenebisacrylamide. The gelation reaction is initiated by ammonium peroxydisulfate. After the mixing of the components, the solutions are filtered with 0.2 $\mu$m filters to get rid of dust particles. Gelation is carried out at 70 °C for 12 h after nitrogen has been bubbled in the solution to remove the dissolved oxygen that would inhibit the radical reaction. The cross-link density, $r_c$, is defined as the molar concentration ratio of bisacrylamide to acrylic acid units.

The ionization degree, $\alpha$, is defined as the ratio of the number of carboxylate groups to the total number of monomers. Since poly(acrylic acid) is a weak acid, $\alpha$ can be varied over a wide range by changing the pH of the medium. In aqueous solution, $\alpha$ has a nonzero value due to the acid–base equilibrium. The ionization degree is a decreasing function of the polymer concentration. For the concentrations of preparation used in this study ($C$ = 1.11 and 1.44 M, where M units stand for mol/L, as usual), the dissociation of the polyacid is very low. Thus, we have approximated the dissociation constant to that of the monomeric acrylic acid: $K_a = 5.6 \times 10^{-5}$. This leads to $\alpha \simeq 7.5 \times 10^{-3}$. Higher ionization degrees ($\alpha > 10^{-2}$) are obtained by partial neutralization of the polyacid with NaOH to a given stoichiometric neutralization degree.

Except for a few gels that were prepared from preneutralized monomers, the samples were prepared in pure aqueous solutions, that is, at an ionization degree $\alpha \simeq 7.5 \times 10^{-3}$. Cylindrical glass tubes were immersed in the initial solution of monomers. Once the gelation was carried out, these tubes were taken out and cylindrical gels were gently pushed out of the tubes with a piston. Using this procedure, it was possible to obtain cylindrical samples with no cracks and the following typical dimensions: 8 cm length and 3–15 mm diameter. These gels were then cut to the desired length and immersed into aqueous NaOH solutions for neutralization.

To investigate the effect of the ionization degree on the elastic properties of the gels at a fixed concentration close to that in the reaction bath, we transferred some samples prepared at $C$ = 1.11 M in cuvettes containing a given amount of NaOH solutions with different pH values such that the final polymer concentration in the gel was $C$ = 1 M. Some of these samples were subsequently swollen by a small amount of NaCl solution. The final polymer concentration was then $C$ = 0.916 M.

For light scattering experiments, it is preferable to study gel samples in contact with the cell walls. Because of this constraint, we prepared the samples assigned to these experiments with a polymer concentration of 0.666 M.

The gels studied at the swelling equilibrium were first neutralized and then put in a large excess of the appropriate solvent (pure water or brine). A most important quantity in charged systems is the screening length of electrostatic interactions, which is usually given by the Debye–Hückel expression $\kappa^2 = 4\pi l_B(\alpha\phi + 2\phi_s)$, where $l_B$ is the Bjerrum length and $\phi$ and $\phi_s$ are the polymer and monovalent salt concentration (in Å$^{-3}$), respectively. Note that throughout this paper we use different notations for concentrations according to their units. For gels at swelling equilibrium in an excess of solvent, the establishment of Donnan equilibrium should in principle be taken into account and $\kappa^2 = 4\pi l_B[(\alpha\phi)^2 + (2\phi_s)^2]^{1/2}$. For most of our experimental conditions, the two definitions give very close values due to the high swelling degrees and the high salt concentrations.

**B. Stress–Strain Measurements.** The shear modulus was obtained from uniaxial compression measurements. The apparatus used and the related experimental procedure have been described elsewhere.[12] The samples were cylindrical gels with the following typical size: length 1 cm, diameter 1 cm. All measurements were carried out at deformation ratios $0.8 \le \lambda \le 1$.

The general stress–strain relation that applies to swollen gels at small deformation is the simplified Mooney–Rivlin equation

$$\sigma = \mu(\lambda - 1/\lambda^2) \tag{1}$$

where $\sigma$ is the stress per unit undeformed area and $\mu$ is the shear modulus. Figure 1 shows plots of the ratio $\sigma/(\lambda - 1/\lambda^2)$ versus $\lambda$ for a series of gels at the swelling equilibrium. As a general rule, the data fit horizontal straight lines except in the range of $\lambda^{-1}$ close to unity, where deviations due to surface effects appear. The data relative to the most swollen gels exhibit a slight positive slope. This will be discussed in the last section of this paper.

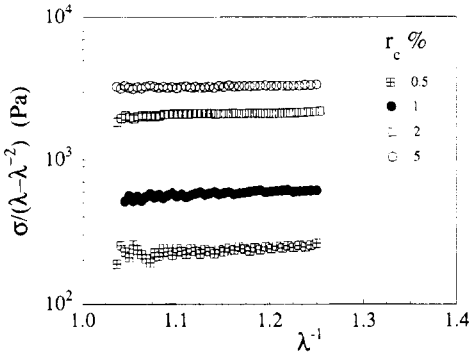


**Figure 1.** Some examples of $\sigma/(\lambda - \lambda^{-2})$ vs $\lambda^{-1}$ plots for ionized gels with varying cross-linking degrees at swelling equilibrium in salted water (see Table 1 for experimental conditions).

**C. Light Scattering Experiments.** The light scattering setup has been described in a previous paper.[15] A device using a stepping motor allows us to translate the scattering cell so that various scattering volumes into the sample can be probed. An automated procedure provides a measure of the count rate for each particular scattering volume during an integration time of 5 s. The sample is translated by steps varying from 3.3 to 25 $\mu$m, the total displacement being 5 mm. Such a device allows one to estimate the ensemble-averaged intensity $\langle I\rangle_E$ and the root mean square fluctuations. These quantities are normalized by the intensity scattered from toluene. The data reported in the following refer to normalized intensities. The coherence factor $\beta$ that is related to the number of coherence areas $n$ over which the scattered light is collected ($\beta \simeq n^{-1/2}$) can be varied by adjusting the size of the pinhole in front of the photomultiplier. This factor can be estimated from dynamic light scattering experiments from a standard scattering medium (latex). These experiments provide the normalized autocorrelation function of the scattered intensity $g^{(2)}(\tau)$ given by

$$g^{(2)}(\tau) = 1 + \beta^2|f(q,\tau)|^2 \tag{2}$$

where $f(q,\tau)$ is the intermediate scattering function and $q$ denotes the scattering wavevector defined in the usual way. In our experiments $\beta$ could be varied between 0.5 and 0.96, the latter value corresponding approximately to a single coherence area detection.

Figure 2 shows the variation of the scattered intensity $\langle I\rangle_T$ when scanning through various positions in a gel with cross-link density $r_c$ = 0.03, degree of ionization $\alpha$ = 0.1, and polymer concentration $C$ = 1.11 M. Also plotted is the intensity scattered from a semidilute solution at the same concentration and degree of ionization. The ensemble-averaged intensity $\langle I_{gel}\rangle_E$ relative to the gel is significantly larger than the intensity $I_{sol}$ scattered from the solution, in agreement with previous findings.[15,16] It was shown that, for a given scattering volume, $I_{gel}$ can be split into two contributions. The first one, $I_C$, arises from frozen fluctuations in polymer concentration and can be considered as constant on the time scale investigated in a dynamic light scattering experiment. The second one, $I_F$, is within experimental accuracy equal to the intensity scattered from the corresponding solution and represents the dynamic fluctuations of concentration in the gel. While $I_F$ is independent of scattering volume, $I_C$ exhibits huge variations when scanning through various locations in the gel and is

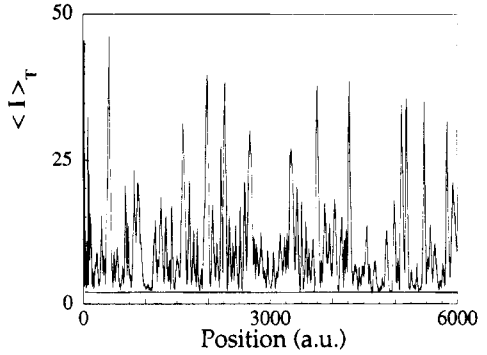


**Figure 2.** Variation of the scattering intensity with position in a gel ($C$ = 1.11 M, $f$ = 0.1, $r_c$ = 0.03) and in the corresponding solution (flat line). The data were recorded during a back and forth displacement as easily seen from the symmetry in the intensity variations.

responsible for the chaotic behavior of $I_{gel}$ depicted in Figure 2. These large variations can be reduced by opening the aperture in front of the photomultiplier and by averaging the scattering intensity over many coherence areas. Data in Figure 2 correspond to a single coherence area detection ($\beta$ = 0.96), which allows one to observe the full amplitude of the frozen intensity fluctuations.

Intensity correlation functions were measured by an ALV-5000 multibit correlator (ALV, Langen, Germany). The device using the stepping motor allows a measure of the time-averaged correlation function $g_T^{(2)}(\tau)$ for each scattering volume probed. The ensemble-averaged intensity correlation function can be calculated by summing the nonnormalized correlation functions and then performing a normalization by the total number of photocounts and the number of summations.[16-18]

**D. Swelling Experiments.** Cylindrical gels with dimensions 3.4 mm diameter and ≃17 mm length are prepared according to the procedure described above. Once the gels are neutralized, they are transferred into a cell containing an excess of solvent. This time is taken to be the time origin $t$ = 0. The diameter of the gel cylinder is measured as a function of time on the screen of a profile projector by using a calibrated scale.

The analysis of the data was performed by using the model proposed by Li and Tanaka.[19,20] At large $t$ the gel diameter $d(t)$ approaches exponentially its equilibrium value according to

$$-\ln \frac{d_f - d(t)}{d_f - d_i} = \frac{t}{\tau_1} - B \tag{3}$$

where $d_f$ and $d_i$ stand for the final and initial diameters, respectively, $\tau_1$ is the relaxation time of the slowest mode in the swelling process, and $B$ is a parameter that depends only on the geometry of the gel and the ratio of the shear modulus $\mu_e$ over the osmotic longitudinal modulus $M_{os}$.

Figure 3 shows a typical swelling kinetics. From eq 3, $B$ can be determined from the short-time linear extrapolation of the logarithmic plot (intercept) and $\tau_1$ from the slope of the straight line. Once the $B$ value is established, the $\mu_e/M_{os}$ value follows, since the dependence of $B$ on $\mu_e/M_{os}$ for spheres, cylinders, and disks has been established numerically and can be found in the literature.[19,20]

The cooperative diffusion coefficient $D_e$ of the gel at the swelling equilibrium is given by

$$D_e = \frac{3}{8}\frac{d_f^2}{\tau_1 X_1^2} \tag{4}$$

where $X_1$ is a known function of $\mu_e/M_{os}$.[19,20] The analysis of the data in Figure 3 leads to the following results: $\tau_1$ = 18750 s, $B$ = 0.22, $\mu_e/M_{os}$ = 0.45, $X_1$ = 2.0, and $D_e = 3.5 \times 10^{-6}$ cm$^2$ s$^{-1}$.

The swelling kinetics of polyelectrolyte gels is very fast. In the absence of salt, an instability, characterized by a wrinkled

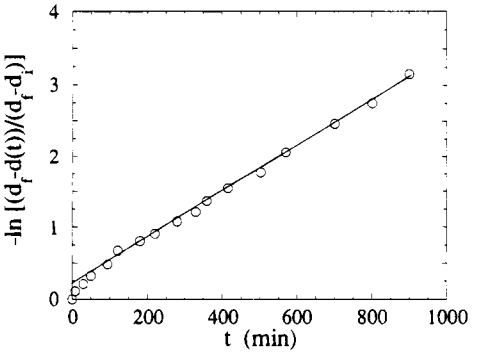


**Figure 3.** Time evolution of the difference between equilibrium diameter and instantaneous diameter during the swelling of a gel with $f$ = 0.35 and $r_c$ = 0.02 in a solution with $C_s$ = 0.117 M. Final diameter of the gel $d_f$ = 8.4 mm.

surface of the gel, is observed at the beginning of the swelling process.[20] In such a case, the concentration profile within the gel is strongly deformed and the theory is not well suited to describe the early stages of the swelling process. As a consequence, the procedure described above gives unrealistic values for the parameter $B$. However, in the final steps, the slope still yields reasonable values for $\tau_1$ that can be used to calculate $D_e$ values since the parameter $X_1$ (eq 4) exhibits only a slight variation with $\mu_e/M_{os}$ in the range of the typical values of this ratio for gels.

## Theoretical Background

The swelling equilibrium of networks, according to the basic Flory–Rehner idea,[3] results from a balance between the osmotic pressure $\Pi_{os}$ acting to swell the network and the elastic pressure due to the stretching of the chains. The rubber elasticity theory assumes that the latter is the simple sum of contributions from changes in the distribution of configurations of individual strands. For a perfect tetrafunctional network without trapped entanglements, the elastic pressure is given by[3]

$$\Pi_{el}/k_BT = A\frac{\phi R^2}{N R_0^2} \tag{5}$$

where $N$ is the number of statistical units between cross-links and $R$ and $R_0$ are the mean-square end-to-end distances of a network strand at the concentration $\phi$ and in its reference state, respectively. The prefactor $A$ depends on the assumption made concerning the fluctuations of the interchain junctions. The phantom network theory, which assumes that the junctions perform a Brownian motion about their mean positions, predicts $A$ = 1/2.[21,22] If, on the contrary, all the junction fluctuations are suppressed due to topological interactions, then one finds $A$ = 1. In any case, this is not a relevant issue in the present study, since it does not aim at comparing quantitatively measured values and theoretical predictions for the thermodynamic parameters.

Also a controversial discussion has been going on over the years about the meaning of $R_0$. In the original Flory theory, the reference state is taken to be the Gaussian one with $R_0^2 = Na^2$, $a$ being the statistical unit length.[3] Then, it was stated that $R_0$ was the mean square end-to-end distance of the strand in the preparation state.[21,22] On the basis of osmotic deswelling results, Bastide et al. proposed a phenomenological scaling approach that does not require a detailed knowledge of the variation upon swelling of the microscopic parameters that characterize the network.[23] More recently, Panyukov[10] and

Obukhov et al.[11] suggested that $R_0$ represents the end-to-end distance the strand would have if it was a free chain of $N$ segments in solution at concentration $\phi$. In fact, the choice of $R_0$ has no drastic consequences for the behavior of gels prepared in the presence of a diluent at a concentration close to the equilibrium one. On the other hand, the issue is highly relevant for gels prepared under $\Theta$ conditions and swollen to a large extent due to a subsequent ionization. The case of polyelectrolyte gels has been recently studied by Barrat et al.[9] They developed a model for polyelectrolytes at the swelling equilibrium in a $\Theta$ solvent of the backbone in the weak screening limit. In this model the reference state of the strand is the Gaussian conformation. In the following we will adopt the same assumption but we will also compare the experimental results with the predictions of the Panyukov–Obukhov et al. model.[10,11]

The osmotic pressure in the polyelectrolyte gels is mainly due to the counterions.[9,24] Its expression depends on the amount of salt in the gel and on the strength of the screening. Different cases have been considered by Barrat et al.[9]

**A. Low Salt Concentration**: $\phi_s \ll \alpha\phi$. In this limit, $\Pi_{os}$ results essentially from the entropy of counterions and is given by[24]

$$\Pi_{os}/k_BT \simeq \left[1 - \frac{l_B}{2\Lambda}\right]\alpha\phi \tag{6}$$

where $\Lambda = b/\alpha$ is the contour length of the chain between two consecutive charges, $b$ being the length of one monomer unit. In the limit of Manning's condensation, $\Lambda = l_B$ and eq 6 becomes independent of $\alpha$:

$$\Pi_{os}/k_BT \simeq \frac{1}{2}\frac{b}{l_B}\phi \tag{7}$$

Equations 6 and 7 are well confirmed qualitatively by direct osmotic pressure measurements.[25] They explain also quite well light scattering measurements in the limit of vanishing wave vector $q$.[12–14]

The equality between osmotic and elastic pressures (eqs 5 and 6) in conjunction with $R_0^2 = Na^2$ leads to the following expression for the end-to-end distance of the strand at the swelling equilibrium:

$$R_e \simeq Na\alpha^{1/2} \tag{8}$$

Therefore the chains are strongly stretched at swelling equilibrium, even at small ionization degree $\alpha$.

The equilibrium swelling concentration $\phi_e$ is given by the packing condition

$$\phi_e \sim NR_e^{-3} \tag{9}$$

which leads to

$$Q_e = a^{-3}\phi_e^{-1} \sim N^2\alpha^{3/2} \tag{10}$$

From eqs 5–10 one obtains the following expressions for the osmotic compressional modulus $K_e$ and the shear modulus $\mu_e$ at the swelling equilibrium:

$$K_e \simeq \mu_e \sim k_BTa^{-3}N^{-2}\alpha^{-1/2} \tag{11}$$

**B. High Salt Content**: $\phi_s \gg \alpha\phi$. In this limit, the properties of the gel depend on the screening range.

**(i) Weak Screening Regime ($\kappa R_e < 1$).** This regime is characterized by a uniform distribution of ions throughout the gel (cf. Figure 4a). The salt concentration inside the gel is smaller than the nominal salt concentration due to the establishment of a Donnan equilibrium between the gel and the surrounding solvent. The resulting osmotic pressure difference between the inside and the outside of the gel, $k_BT\alpha^2\phi^2/4\phi_s$, is balanced against the elastic restoring force to give

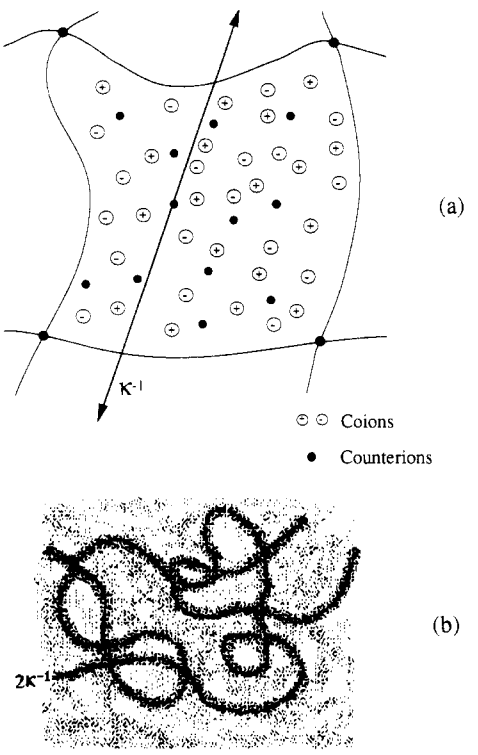


**Figure 4.** Sketch of the two different screening regimes for an ionized gel at swelling equilibrium in the presence of salt excess ($2\phi_s \gg \alpha\phi$): (a) weak screening, $\kappa R_e < 1$ (small ions are uniformly distributed in the gel); (b) strong screening, $\kappa R_e > 1$ (small ions form a sheath around the chains; their density is depicted by different gray levels).

$$Q_e = a^{-3}\phi_e^{-1} \sim a^{-4/5}N^{4/5}\left[\frac{\alpha^2}{4\phi_s}\right]^{3/5} \tag{12}$$

where the packing condition (9) has still been used. As for the elastic moduli, they are given by

$$K_e \simeq \mu_e \sim k_BTa^{-12/5}N^{-8/5}\left[\frac{\alpha^2}{4\phi_s}\right]^{-1/5} \tag{13}$$

Barrat et al. have also studied the collective diffusion in the gel in the long-wavelength limit by using a two-fluid model. The collective diffusion $D_e$ at the swelling equilibrium is given by[9]

$$D_e = \frac{\mu_e R_e^2}{\eta_0} \tag{14}$$

where $\eta_0$ is the viscosity of the solvent. Combining eqs 12–14 leads to

$$D_e \sim \frac{k_BT}{\eta_0}a^{-8/5}N^{-2/5}\left[\frac{\alpha^2}{4\phi_s}\right]^{1/5} \tag{15}$$

**(ii) Strong Screening Regime ($\kappa R_e > 1$).** In this regime, both the monomers and the counterions are not uniformly distributed throughout the gel. One can consider the chains as surrounded by a sheath of

countercharges of thickness $\kappa^{-1}$ (Figure 4b). In that case, the contribution to the swelling pressure arising from the fluctuations in the monomer density can become nonnegligible as compared to that due to the Donnan equilibrium. In the limit of high ionic strength, the properties of the gel are similar to those of a usual Flory gel with an electrostatic excluded volume[24]

$$v_e = 4\pi l_B(\alpha^2/\kappa^2) \tag{16}$$

For such a gel the equilibrium swelling degree is given by the $C^*$ theorem[26-28]

$$\phi_e \sim N^{-4/5} a^{-6/5} v_e^{-3/5} \tag{17}$$

$$Q_e \sim a^{-9/5}(4\pi l_B)^{3/5} N^{4/5}(\alpha/\kappa)^{6/5} \tag{18}$$

It can be noted that relation 18 coincides with relation 12 even though they describe different physical situations represented in Figure 4a and Figure 4b, respectively. It could be argued that the situation encountered in the case of high ionic strength (Figure 4b) mimics on a more microscopic scale the Donnan equilibrium that plays the major role in the weak screening limit. Such an analogy was proposed earlier[29] and might explain the identity of eqs 12 and 18. Moreover, eq 10 can be recovered easily by setting $\phi_s = 0$ into the expression for $\kappa$ in eq 18. This suggests that the latter equation could also be a good approximation to describe intermediate salt concentration conditions.

Several remarks can be made with respect to the above statements.

(i) For weakly charged gels, one cannot neglect the usual virial contribution to the osmotic pressure so that the effective excluded volume becomes for a Θ solvent

$$v_{eff} = v_e + 2v\tau_r + 3w\phi \tag{19}$$

where $v$ is the excluded volume of the neutral polymer, $w$ is the third virial coefficient, and $\tau_r$ is the reduced temperature with respect to the Θ temperature.

(ii) In the presence of a large excess of salt, typically when $\kappa^{-1} < l_B$, the Debye–Hückel theory is no longer valid and one should recover the behavior of a neutral polymer. As most of the polyelectrolytes have a hydrophobic backbone, one should observe a Θ solvent behavior.

(iii) Although eq 17 is the same as for neutral gels, it must be kept in mind that as long as we are not in the preceding limit of a very large excess of salt, the excluded volume parameter $v_e$ depends on the polymer concentration through eq 16. Therefore, the concentration dependences of the thermodynamic parameters are different for neutral and charged gels.

Expressions for the elastic moduli can be derived from the osmotic pressure. If we assume that the Donnan equilibrium is the dominant mechanism, $\Pi_{os}$ is given by[9]

$$\Pi_{os}/k_BT \simeq \alpha^2\phi^2/4\phi_s \tag{20}$$

which, in the limit $\phi_s \gg \alpha\phi$, can be approximated by

$$\Pi_{os}/k_BT \simeq \frac{1}{2}v_e\phi^2 \tag{21}$$

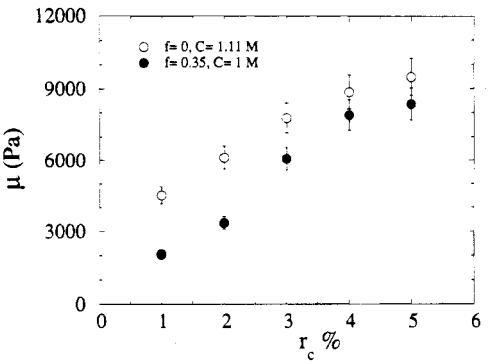


**Figure 5.** Variation with cross-linking degree of the shear modulus for two gels with different ionization degrees and close to their concentration in the reaction bath.

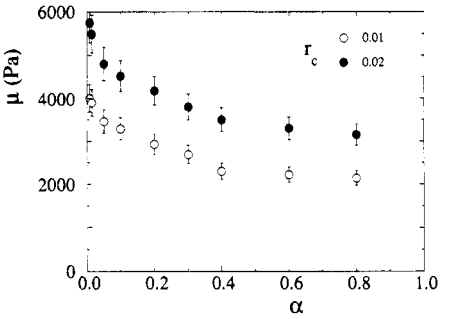


**Figure 6.** Influence of neutralization on the shear modulus for two series of gels with different cross-linking degrees ionized after the gelation ($C$ = 1 M, $C_s$ = 0 M).

The above relationship is valid for ionic strengths small enough that the dominant contribution to the osmotic pressure results from the electrostatic excluded volume.

Within this approximation, the elastic moduli and the cooperative diffusion coefficient are given by

$$K_e \simeq \mu_e \sim k_BTa^{-12/5}(4\pi l_B)^{-1/5}N^{-8/5}(\alpha/\kappa)^{-2/5} \tag{22}$$

$$D_e \sim \frac{k_BT}{\eta_0}a^{-8/5}(4\pi l_B)^{1/5}N^{-2/5}(\alpha/\kappa)^{2/5} \tag{23}$$

which are equivalent to (13) and (15) in the limit $\phi_s \gg \alpha\phi$.

## Experimental Results

**A. Gels in the Reaction Bath.** We consider here both nonneutralized samples at the concentration of preparation and samples at a slightly lower concentration prepared by means of the procedure described in the Experimental Section in order to neutralize the gels or to incorporate some salt.

Figure 5 shows the variation of the shear modulus with $r_c$ for quasi-neutral gels ($\alpha \simeq 7.5 \times 10^{-3}$) and gels with an ionization degree $\alpha = 0.35$. The shear modulus of quasi-neutral gels is found to be significantly larger than that of the charged ones, except at high cross-link density where there is only a slight difference that can be accounted for simply by the small concentration difference. The effect of the ionization degree on the shear modulus is illustrated in Figure 6 relative to two series of gels with different cross-link densities. Obviously, this effect has to deal with electrostatic interactions since the screening of these interactions by addition of salt produces an increase of the shear modulus that tends to recover the value of the quasi-neutral gels

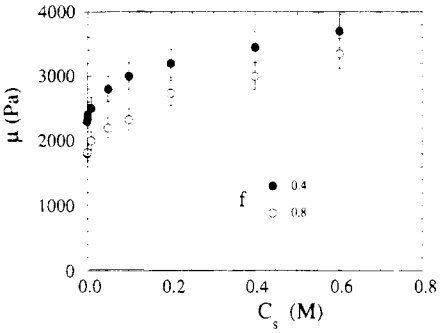


**Figure 7.** Influence of salt addition on the shear modulus for two series of gels with different neutralization degrees. Gels are first neutralized and then swollen in salted solutions (final concentration $C = 0.916$ M). Cross-linking ratio is constant: $r_c = 0.02$.

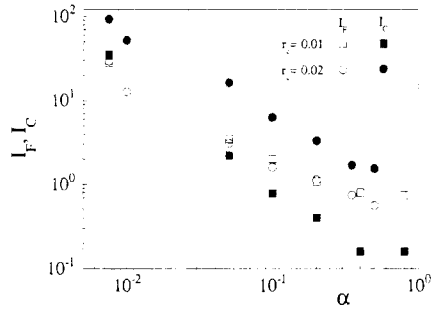


**Figure 8.** Effect of the ionization degree on the frozen (closed symbols) and fluctuating (open symbols) contributions to the scattering intensity. Squares: gels neutralized prior to the gelation ($C = 1.11$ M, $r_c = 0.01$). Circles: gels neutralized after the gelation ($C = 1$ M, $r_c = 0.02$). Ionization degrees are calculated without taking into account Manning's condensation at high neutralization degree (see text).

(Figure 7). Results similar to those of Figure 6 have been reported by Ilmain et al. for both gels prepared from ionized monomers and gels subsequently ionized after preparation, thus demonstrating that this effect is not simply due to a change of network topology with the ionization degree of the monomers.[12,30]

In Figure 8 are plotted the frozen component, $I_C$, and the fluctuating contribution, $I_F$, for two gels with different $r_c$ as a function of the neutralization degree $f$. One of the gels ($r_c = 0.01$) was synthesized with preneutralized monomers, while the second one ($r_c = 0.02$) was neutralized after the gelation. In both cases the frozen-in contribution is reduced by an increase of the ionization degree. It is not possible from these results to draw a conclusion on the relative effect of the neutralization prior to or after the gelation because polymer concentration and cross-link density are different. A recent study by small-angle neutron scattering (SANS) suggests that the effect of ionization degree on the frozen-in fluctuations is enhanced if the neutralization is performed prior to the gelation.[31] Let us mention also that $I_C$ is enhanced by an increase of $r_c$.[31] In the case of small cross-linking degree, the frozen contribution is found to become smaller than the fluctuating component for large enough ionization degrees.

**B. Gels at Swelling Equilibrium.** Figure 9 shows the effect of the cross-link density on the equilibrium swelling degree $Q_e$ of gels prepared at a polymer concentration $C = 1.11$ M, subsequently neutralized to reach an ionization degree $\alpha = 0.35$. Salt concentration is kept equal to $C_s = 0.171$ M (1 g/L). In Figure 10 is reported the variation of the shear modulus $\mu_e$ of these gels at the swelling equilibrium as a function of $r_c$.

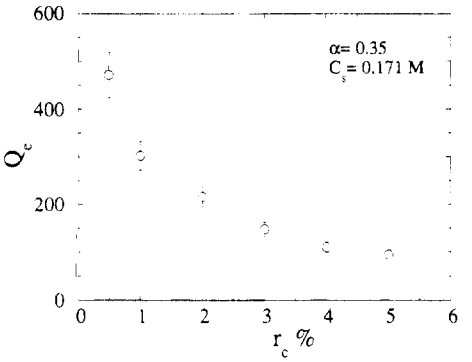


**Figure 9.** Swelling equilibrium ratio versus cross-linking ratio. Gels are ionized after the reaction (Table 1).

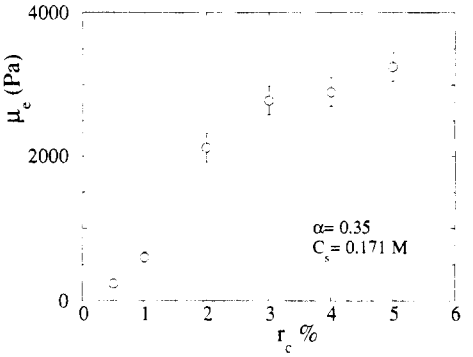


**Figure 10.** Shear modulus at swelling equilibrium versus cross-linking ratio for the same samples as in Figure 9.

**Table 1. Equilibrium Properties of Gels Neutralized after Synthesis ($f = 0.35$, $C_s = 0.171$ M): Effect of Cross-Link Density**

| $r_c$ (%) | $Q_e$ | $\mu_e$ (Pa) | $D_e$ ($10^{-6}$ cm$^2$/s) | $\mu_e/M_{os}$ | $\kappa^{-1}$ (Å) |
|---|---|---|---|---|---|
| 0.5 | 472 | 240 | 1.0 | | 19.9 |
| 1 | 302 | 600 | 1.41 | | 18.6 |
| 2 | 216 | 2120 | 3.5 | 0.45 | 17.5 |
| 3 | 148 | 2780 | 4.1 | 0.53 | 16 |
| 4 | 110 | 2900 | 5.8 | 0.59 | 14.7 |
| 5 | 95 | 3250 | 10 | 0.67 | 14 |

Qualitatively, one observes the same trends as in the neutral gels with respect to the effect of $r_c$ on $Q_e$ and $\mu_e$.

The results of the experiments performed on gels with different ionization degrees and salt contents are given in Tables 2–4. The general behavior is that previously reported.[12,13,30] In particular, the equilibrium swelling degree increases upon increasing α or decreasing the salt content. This behavior will be discussed in the next section.

Turning now to the dynamic properties, we have first proceeded to a comparison between the kinetics of swelling and dynamic light scattering experiments. One of the problems encountered concerns the analysis of the dynamic light scattering experiments in gels. Two schemes have been considered up to now.

The first one assumes that the frozen-in fluctuations arise from the presence of static inhomogeneities whereas the dynamic field associated with long-wavelength dynamic density fluctuations is of same nature as in polymer solutions.[32–34] In that case, the intensity autocorrelation function can be treated in terms of a heterodyne mixing between these two components. For neutral gels, this leads to values of $D_e$ close to those obtained in semidilute solutions.[27] Also a good agreement was found between the results of dynamical light scattering obtained using this analysis and those of kinetics of swelling.[20]

**Table 2. Equilibrium Properties of Gels Neutralized after Synthesis ($r_c$ = 0.02): Effect of Ionization and Salt Content**

| $f$ | $C_s$ (g/L) | $Q_e$ | $\mu_e$ (Pa) | $D_e$ ($10^{-6}$ cm$^2$/s) | $\mu_e/M_{os}$ | $\kappa^{-1}$ (Å) |
|---|---|---|---|---|---|---|
| 0.1 | 0 | 360 | 3600 | 4.6 | 0.45 | 64.4 |
| | 0.2 | 170 | 2800 | 2.2 | 0.45 | 33.6 |
| | 0.5 | 110 | 2900 | 1.5 | 0.45 | 24.1 |
| | 1 | 70 | 3300 | 1 | 0.47 | 17.9 |
| | 2.5 | 46 | 3800 | 0.8 | 0.5 | 12.3 |
| | 5 | 30 | 4400 | 0.4 | 0.48 | 9.1 |
| | 10 | 22 | 4900 | 0.33 | 0.5 | 6.7 |
| | 25 | 10 | 6900 | | | 4.3 |
| 0.2 | 0 | 450 | 3900 | 12 | 0.45 | 50.9 |
| | 0.2 | 210 | 2700 | 6.9 | 0.45 | 28.9 |
| | 0.5 | 150 | 2600 | 5.4 | 0.45 | 21.8 |
| | 1 | 106 | 2800 | 3.6 | 0.45 | 16.9 |
| | 2.5 | 70 | 3200 | 2.2 | 0.46 | 11.8 |
| | 5 | 50 | 3600 | 1.3 | 0.46 | 8.8 |
| | 10 | 38 | 4200 | 0.8 | 0.45 | 6.6 |
| | 25 | 16 | 5500 | 0.4 | 0.46 | 4.2 |
| | 50 | 9 | 6900 | | | 3 |
| 0.35 | 0 | 980 | 4100 | 16 | 0.43 | 56.8 |
| | 0.2 | 480 | 2800 | 11.2 | 0.44 | 31.5 |
| | 0.5 | 350 | 2500 | 8 | 0.45 | 23.6 |
| | 1 | 240 | 2300 | 4.6 | 0.47 | 17.9 |
| | 2.5 | 150 | 2300 | 3.4 | 0.45 | 12.2 |
| | 5 | 108 | 2500 | 3 | 0.48 | 9.1 |
| | 10 | 75 | 3000 | 2.1 | 0.5 | 6.6 |
| | 25 | 40 | 4200 | 1.1 | 0.53 | 4.2 |
| | 50 | 13 | 6400 | | | 3 |

**Table 3. Swelling Equilibrium Degree of Gels Neutralized after Synthesis ($r_c$ = 0.01): Effect of Ionization and Salt Concentration**

| $C_s$ | $f$ = 0.1 | | $f$ = 0.2 | | $f$ = 0.3 | | $f$ = 0.4 | |
|---|---|---|---|---|---|---|---|---|
| (g/L) | $Q_e$ | $\kappa^{-1}$ (Å) | $Q_e$ | $\kappa^{-1}$ (Å) | $Q_e$ | $\kappa^{-1}$ (Å) | $Q_e$ | $\kappa^{-1}$ (Å) |
| 0 | 1205 | 118 | 1790 | 102 | 2680 | 101 | 3970 | 107 |
| 0.1 | 572 | 54.3 | 850 | 50.6 | 1250 | 50.3 | 1890 | 51.9 |
| 0.2 | 390 | 41 | 570 | 38.4 | 840 | 38.2 | 1067 | 37.8 |
| 0.5 | 260 | 28.1 | 380 | 26.8 | 560 | 26.7 | 875 | 27.4 |
| 1 | 175 | 20.6 | 260 | 19.9 | 377 | 19.8 | 625 | 20.3 |
| 2.5 | 102 | 13.5 | 173 | 13.7 | 255 | 13.3 | 410 | 13.5 |
| 5 | 66 | 9.7 | 100 | 9.5 | 166 | 9.6 | 260 | 9.7 |
| 10 | 60 | 7 | 70 | 6.9 | 90 | 6.8 | 150 | 6.9 |
| 25 | 37 | 4.5 | 55 | 4.5 | 70 | 4.5 | 90 | 4.5 |
| 50 | 25 | 3.2 | 43 | 3.2 | 53 | 3.2 | 66 | 3.2 |

**Table 4. Swelling Equilibrium Degree of Gels Prepared from Neutralized Monomers ($r_c$ = 0.005): Effect of Ionization and Salt Content**

| $C_s$ | $f$ = 0.2 | | $f$ = 0.3 | | $f$ = 0.4 | | $f$ = 0.5 | |
|---|---|---|---|---|---|---|---|---|
| (g/L) | $Q_e$ | $\kappa^{-1}$ (Å) | $Q_e$ | $\kappa^{-1}$ (Å) | $Q_e$ | $\kappa^{-1}$ (Å) | $Q_e$ | $\kappa^{-1}$ (Å) |
| 0 | 2640 | 131 | 3050 | 115 | 3760 | 110 | 4407 | 106 |
| 0.1 | 1200 | 56.6 | 1464 | 54.1 | 1790 | 53 | 2233 | 52.7 |
| 0.5 | 460 | 28.2 | 695 | 28.3 | 830 | 27.8 | 1090 | 27.9 |
| 1 | 280 | 20.5 | 360 | 20.1 | 470 | 20 | 580 | 19.9 |
| 5 | 120 | 9.8 | 170 | 9.7 | 204 | 9.7 | 270 | 9.7 |
| 10 | 75 | 7 | 108 | 7 | 150 | 7 | 194 | 7 |
| 50 | 26 | 3.2 | 60 | 3.2 | 96 | 3.2 | 170 | 3.3 |
| 100 | 4.7 | 2.1 | 15 | 2.2 | 30 | 2.3 | 64 | 2.3 |
| 200 | | | 4.7 | 1.6 | 4.7 | 1.5 | 11 | 1.6 |

In a second approach, the gel is considered as an arbitrary nonergodic medium and one measures an intermediate scattering function whose initial decay provides a diffusion constant that takes into account the ensemble of the density fluctuations in the gel. This diffusion constant is found to be much lower than that measured assuming the heterodyne scheme.[16,18,35] In fact, it seems that this low value could reflect as well an averaging of fast cooperative fluctuations in polymer concentration and of very slow motion of inhomogeneities. However, the model is not yet suited to account for that effect.

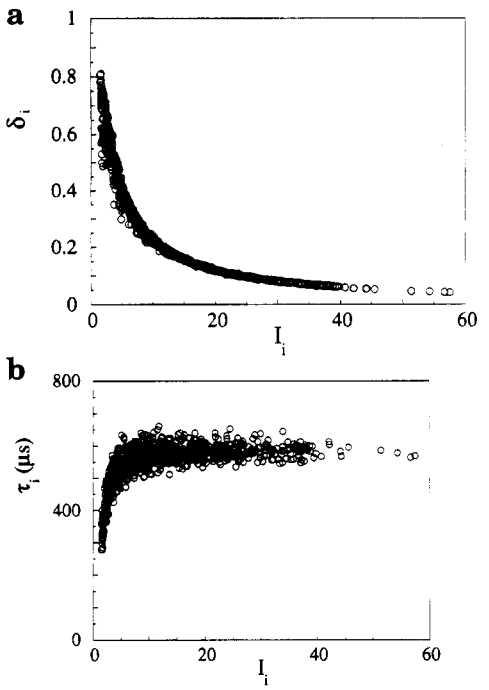


**Figure 11.** (a) Variation of the amplitude of the intensity autocorrelation function as a function of the scattering intensity when scanning different positions in a gel with $C$ = 1.11 M, $f$ = 0, and $r_c$ = 0.02. (b) Variation of the decay time of the intensity autocorrelation function as a function of the scattering intensity (same conditions as in (a)).

We measured the time-averaged intensity correlation function $g_T^{(2)}(\tau)$ over a set of 997 scattering volume positions with an aperture of the detector such that $\beta$ = 0.96 for a gel with $C$ = 1.11 M, $\alpha = 7.5 \times 10^{-3}$, and $r_c$ = 0.02. When scanning over various positions $i$, the normalized functions $g_T^{(2)}(\tau)$ can be approximated by $1 + \delta_i \exp(-t/\tau_i)$, where $\delta_i$ decreases upon increasing the intensity $I_i$ scattered by the corresponding scattering volume. Figure 11 shows the variations of $\delta_i$ and $\tau_i$ as a function of $I_i$. It can be seen that $\tau_i$ varies between a lower value $\tau_s$ for the lowest values of $I_i$ to a higher value of $2\tau_s$ as $I_i$ becomes large. These two limits correspond to dark and bright speckles, respectively. The same behavior is observed for all scattering angles investigated ($20° \leq \theta \leq 135°$).

A critical test to discriminate between the heterodyne mixing and the nonergodic hypothesis is the angular dependence of the contributions $I_F$ and $I_C$.[35] In our experiments these two contributions are independent of scattering angle within experimental accuracy, which favors the hypothesis of heterodyne mixing of the fluctuating component by the static intensity scattered from small regions (<300 Å) with larger concentration.

The method described above gives diffusion coefficient values in good agreement with the ones obtained from the swelling kinetics. As an example, for a gel ionized after the gelation ($\alpha$ = 0.35, $r_c$ = 0.02, $C_s$ = 0.171 M), we measure by dynamic light scattering $D = (4.0 \pm 0.3) \times 10^{-6}$ cm$^2$ s$^{-1}$ ($Q$ = 200 ± 20) while the kinetics of swelling yields $D_e = (4.6 \pm 0.6) \times 10^{-6}$ cm$^2$ s$^{-1}$ ($Q_e$ = 240 ± 25). Considering the difference in concentrations, the agreement is quite satisfactory. Thus kinetics of swelling experiments are well suited to measure the diffusion constant at swelling equilibrium, i.e., when light scattering requires tedious matching of gel sizes. Furthermore, the experiments of kinetics of swelling provide an estimate of the ratio $\mu_e/M_{os}$ (cf. Experimental

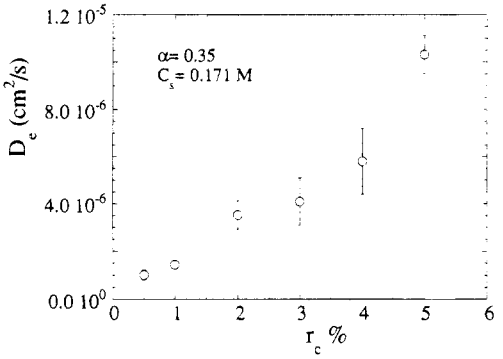


**Figure 12.** Influence of cross-linking degree on the cooperative diffusion coefficient measured by the kinetics of swelling (data from Table 1).

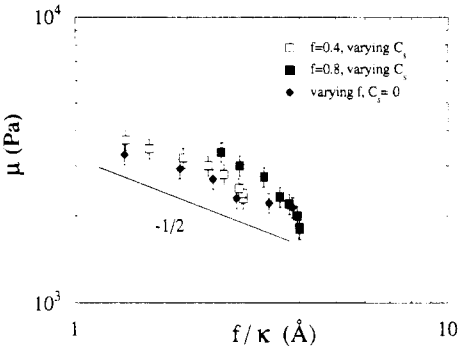


**Figure 13.** Variation of the shear modulus with the parameter $\alpha/\kappa$. Gels ionized after the reaction. Squares: gels containing added salt ($C = 0.916$ M). Diamonds: gels without added salt ($C = 1$ M). Cross-linking ratio is constant: $r_c = 0.01$.

Section). Measured values of $D_e$ and $\mu_e/M_{os}$ are reported in Tables 1, and 2.

Qualitatively, the effect of the cross-linking degree on $D_e$ is the same as for neutral gels; namely, $D_e$ increases with $r_c$ (Figure 12). Also, the behavior upon a variation of ionization degree and/or salt content is that already reported for gels in the reaction bath, i.e., an increase of $D_e$ upon increasing $\alpha$ and/or decreasing $C_s$.[12,30]

## Discussion

**A. Gels in the Reaction Bath.** According to eq 5, for such gels one would expect the shear modulus to be proportional to the cross-link density. Therefore, the shear modulus at a given polymer concentration should be proportional to $r_c$ if the cross-linkers were randomly distributed throughout the sample. This is not what is observed in Figure 5 for quasi-neutral gels. In fact, this is not surprising since it is well known for neutral gels that the occurrence of topological defects like trapped entanglements and free dangling chains can modify the behavior of the shear modulus. Moreover, it has been shown that the gels prepared by radical copolymerization exhibit submicroscopic inhomogeneities whose effect on the thermodynamic properties of gels is not totally elucidated.

More surprising is the decrease of the shear modulus upon increasing the ionization degree (Figure 6) and the subsequent increase of $\mu$ as electrostatic interactions are progressively screened by addition of salt (Figure 7). Since the cross-linking degree remains constant in these experiments, the explanation for these behaviors is to be found in more subtle effects.

A possible explanation is provided by the model of Panyukov and Obukhov et al., which states that $R_0$ must be taken as the end-to-end distance the strand would have in a solution at the same concentration.[10,11] Thus, $R_0^2$ should increase with $\alpha$ because of the swelling of the chains by electrostatic interactions. The mean square end-to-end distance of a chain swollen by the electrostatic excluded volume $v_e$ in a semidilute solution is[26]

$$R_0^2 \sim Na^{1/2}v_e^{1/4}\phi^{-1/4} \tag{24}$$

$$R_0^2 \sim Na^{1/2}(4\pi l_B)^{1/4}(\alpha/\kappa)^{1/2}\phi^{-1/4} \tag{25}$$

Assuming that the average position of the cross-links is not affected by a variation of $\alpha$ so that $R^2 = Na^2$ remains unchanged, one finds using eq[25]

$$\mu \sim k_B T N^{-1} a^{3/2}(4\pi l_B)^{-1/4}(\alpha/\kappa)^{-1/2}\phi^{5/4} \tag{26}$$

Figure 13 shows the variation of $\mu$ as a function of $f/\kappa$. For the data corresponding to $f \leq 0.4$ one can assume $f \approx \alpha$. On the other hand, for the data obtained on the sample with $f = 0.8$, $\alpha/\kappa$ would be smaller than $f/\kappa$ due to Manning condensation. Indeed inspection of the data in Figure 6 shows that increasing neutralization has little effect on the shear modulus once $f \geq 0.4$. A similar effect is observed for the influence of neutralization degree on the two components of the scattering intensity (Figure 8). Taking into account counterion condensation, one can consider by inspection of Figure 13 that $\alpha/\kappa$ is the relevant variable. The square root variation of $\mu$ with $\alpha/\kappa$ is rather well obeyed in spite of the downturn for high values of $\alpha/\kappa$, and one can admit that, qualitatively, the behavior of $\mu$ as a function of $\alpha$ can be explained by the model of Panyukov and Obukhov et al.[10,11] Also the linear variation of $\mu$ with $r_c$ for large $\alpha$ (Figure 5) is in agreement with eq 26. However, the model does not account easily for the weak sensitivity of $\mu$ to $\alpha$ at high cross-link densities (cf. Figure 5).

An alternate explanation for the effect of $\alpha$ on $\mu$ can be proposed on the basis of a modification of the submicroscopic structure of the gel under a change of the ionization degree, as sketched in Figure 14.

Under preparation conditions the gels are slightly charged ($\alpha \simeq 10^{-2}$). Light scattering and SANS experiments have revealed in partially charged gels the presence of static spatial concentration fluctuations.[15,18,31] The range of these fluctuations was found to be much smaller than in neutral gels, and this was interpreted as due to the counterion entropy penalty that would result from the formation of large inhomogeneities.[36,37] Also it was shown that these inhomogeneities are quite dense.[18,31] Therefore, one can consider in a first approximation the gel as a two-phase medium formed of flexible chains connecting dense regions (Figure 14a). In these regions, some of the chains are trapped in between fixed cross-links, while others are held together by interactions between the hydrophobic acid backbones.

Upon ionization the chains rearrange themselves as far as possible. Those of the chains in the dense regions that are free to do it move apart to give a new structure as sketched in Figure 14b. Addition of salt produces a screening of the interactions, and one recovers the structure depicted in Figure 14a. The structural changes of the gels upon ionization can be monitored by scattering experiments. A peak appears in the structure factor measured by SANS.[12,13,18,31] Also the frozen-in component of the scattered intensity, which reflects the presence of dense regions, is strongly reduced by the presence of electrical charges (Figure 8).

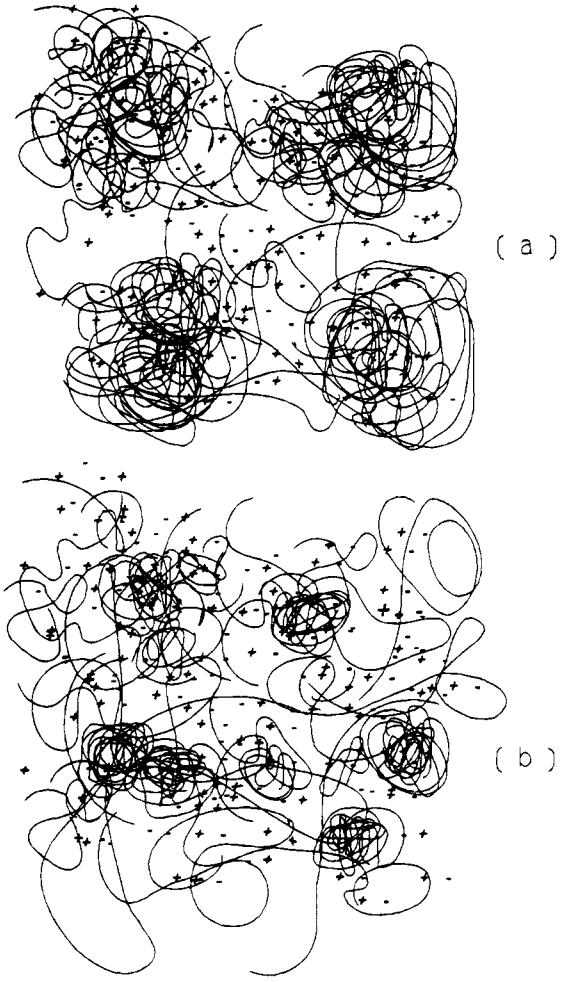


**Figure 14.** Schematic picture for the evolution of gel structure in the reaction bath with the introduction of electrostatic interactions: (a) small ionization degree; (b) large ionization degree.

Obviously, the shear modulus measured experimentally represents an averaged quantity where both individual chains and dense regions contribute. It seems quite likely that the relative weight of these contributions changes upon ionization. In fact, at high ionization degree the gel is much more homogeneous. It is significant in this respect that the shear modulus of ionized gels is a linear function of $r_c$ except at high cross-link density (Figure 5). When $r_c$ is very large, the concentration fluctuations are almost totally frozen-in as shown by light scattering. This result seems to indicate that the dense regions pictured in Figure 14a have invaded the whole space so that the structure of the gel becomes insensitive to the ionization degree. This would explain why $\mu$ is almost independent of $\alpha$ at high $r_c$.

The ionization procedure, i.e., the preneutralization or postneutralization, should also affect the behavior of the shear modulus, since the extent of the frozen-in fluctuations seems to be reduced when the neutralization is performed prior to gelation, as inferred from SANS experiments.[31] We have not made a systematic study on gels prepared according to the two ionization procedures. However, we found the following results for gels with $C = 1$ M, $r_c = 0.02$, and $\alpha = 0.35$. For the gel prepared from ionized monomers, $\mu = 3100 \pm 200$ Pa, while for the gel ionized after preparation, $\mu = 3360 \pm 200$ Pa. Its seems that the shear modulus is slightly larger in the second case but this effect is almost at the limit of experimental error. Moreover, one cannot exclude a slight change in gel architecture due to differences in chemical reactivity for charged and uncharged monomers. At swelling equilibrium, however, differences seem more visible since the gel prepared from ionized monomers has a slightly smaller shear modulus ($Q_e = 224 \pm 20$, $\mu_e = 1800 \pm 200$ Pa) than the gel neutralized after preparation ($Q_e = 240 \pm 25$, $\mu_e = 2300 \pm 200$ Pa).

**B. Gels at the Swelling Equilibrium.** To interpret the results, it is important to have some information on the screening range in the investigated gels. It seems that most of our results have been obtained in a strong screening regime as inferred from the following observations. Let us consider for instance the gels with $r_c = 0.02$. If the cross-links were randomly distributed and if the gel was free of defects, the average number of monomeric units $N$ in between two consecutive cross-links would be about 25. For a gel with an ionization degree $\alpha = 0.35$ swollen at equilibrium in pure water, the chains can be considered to have a stretched conformation. Taking $a = 9$ Å for the statistical unit length and $b = 2.5$ Å as the monomer length, we would get an end-to-end distance of about 60 Å. This is the same order of magnitude as $\kappa^{-1}$ in these conditions (Table 2). Thus, in pure water, we have $\kappa R_e \simeq 1$ for the gels at swelling equilibrium. In fact, two partly compensating errors are not taken into account in this rough estimation: chains are likely not fully stretched but, on the other hand, the effective $N$ value is probably larger than 25 due to defects in the network (see below). Now, in the low-swelling range in the presence of a large excess of salt, the end-to-end distance of the same chain in its Gaussian conformation is reduced to about 23 Å. In that case, $\kappa^{-1}$ values are much smaller (Table 2) and the $\kappa R_e$ value can increase up to about 10. Thus it seems that, in the whole swelling range, the inequality $\kappa R_e \geq 1$ is always fulfilled. The same conclusions can be reached for the smaller cross-linking degrees since the increase of $\kappa^{-1}$ at swelling equilibrium in pure water (Tables 2 and 4) is compensated by an increase in $N$.

As a matter of fact we have seen in the theoretical section that the expression (18) obtained for the strong screening regime still applies in the weak screening regime and crosses over smoothly to the case where no added salt is present (eq 10). However, one possible difficulty concerns the systems for which the number of counterions is approximately equal to that of the salt ions. In this case, the osmotic pressure resulting from the Donnan equilibrium leads to a rather complex expression for $Q_e$, which we tentatively approximate by eq 18. In doing so we underestimate the osmotic pressure by a factor which is at the maximum 1.6 for $\alpha\phi \simeq 2\phi_s$, but we cannot discard in this range of ionic strength the effect of the direct electrostatic interactions[38] and the effect of the non-Gaussian behavior of the elasticity.[39] Another problem can arise in the other limit of very high salt content, where one expects deviations due to a nonnegligible contribution of the chains to the osmotic pressure compared to the ionic pressure. However, recent light scattering experiments performed on PAA gels show that the ionic contribution is dominant in the range of ionic strengths investigated in the present study.[12,13]

From the above discussion, it seems that our results have been obtained in experimental conditions where $\kappa R_e > 1$. Therefore the equations derived in the strong screening limit should apply with a possible restriction

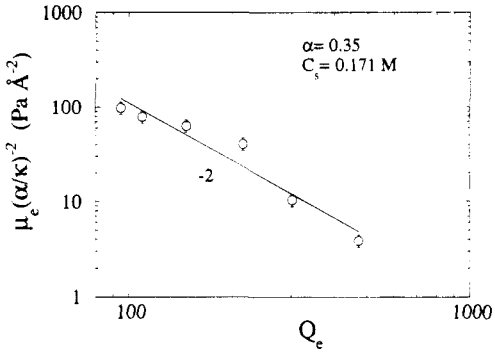


**Figure 15.** Shear modulus as a function of equilibrium swelling ratio in the representation of eq 27. Neutralization degree and salt content are kept constant while cross-linking degree is varied (same samples as in Figure 9). The straight line shows the predicted slope.

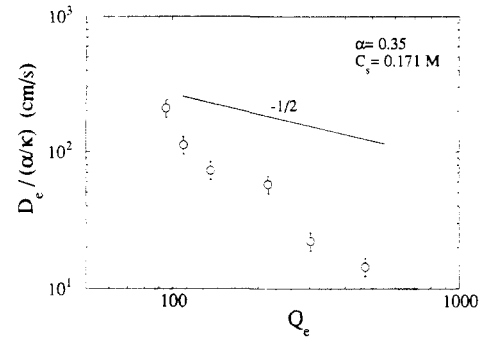


**Figure 16.** Cooperative diffusion coefficient as a function of equilibrium swelling ratio in the representation of eq 28 (same samples as in Figure 9). The straight line corresponds to the expected slope.

for the cases where the salt concentration is not much larger than the counterion concentration. However, since these theoretical expressions crossover smoothly to the no added salt conditions, it is tempting to still use them as approximations. We examine now successively the effect of the cross-link density and that of the electrostatic screening.

**Effect of the Cross-Link Density.** If the gels were defect free and homogeneous, one would expect that $r_c \sim N^{-1}$ and therefore we would have a possible check by comparing the data to the predictions of eqs 18 and 22 relative to the equilibrium swelling degree and the shear modulus. In fact, it appears generally preferable to test the theory by examining the correlation between two macroscopic parameters, since this allows one to eliminate $N$, which is known to vary in a nonsimple way with $r_c$ because of trapped entanglements and dangling chains. By combining eqs 18 and 22, one obtains

$$\mu_e \sim k_B T a^{-6}(4\pi l_B)(\alpha/\kappa)^2 Q_e^{-2} \qquad (27)$$

Figure 15 shows the variation of the product $\mu_e(\alpha/\kappa)^{-2}$ with $Q_e$ in log–log coordinates for gels with varying cross-linking degree (Table 1). We have also drawn through the data a straight line with a slope −2. The agreement is not very good but again, the frozen-in fluctuations might affect the behavior of $\mu_e$. In this respect it must be noted that these static fluctuations, even though they are reduced upon swelling, still remain strongly dependent on the cross-link density.[15]

Similarly, one can combine eqs 18 and 23 to eliminate the dependence on $N$ and obtain

$$D_e \sim \frac{k_B T}{\eta_0} a^{-5/2}(4\pi l_B)^{1/2}(\alpha/\kappa) Q_e^{-1/2} \qquad (28)$$

Figure 16 shows the variation of $D_e(\alpha/\kappa)^{-1}$ as a function of $Q_e$. The predicted decrease of this parameter with $Q_e$ is observed but the variation is larger than the $Q_e^{-1/2}$ theoretical expectation. A fit through the data would yield a much larger slope of about −1.4. From the swelling kinetics experiments one can also measure the parameter $\mu_e/M_{os}$ (see Experimental Section). Since, at swelling equilibrium, $K_e \simeq \mu_e$, one expects $\mu_e/M_{os} \simeq 3/7$. This is a value slightly lower than the results reported in Table 1. Also the ratio $\mu_e/M_{os}$ seems to increase with $r_c$. This could be explained again with the effect of the submicroscopic structure of the gels. The compressional modulus depends essentially on the entropy of counterions whereas the shear modulus might be affected by the presence of inhomogeneities. However, $\mu_e/M_{os}$ values derived from swelling kinetics experiments might also be erroneous when $D_e$ values are about $10^{-5}$ cm$^2$ s$^{-1}$, because then collective motion of the chains proceeds at about the same rate as the restoration of the Donnan equilibrium. The same remark applies to the determination of $D_e$. This point is discussed later on.

**Effect of the Electrostatic Screening.** Equations 18 and 22 predict that, for a given cross-link density, the equilibrium swelling degree and the shear modulus at the equilibrium follow scaling laws of the parameter $\alpha/\kappa$. In Figure 17 are reported sets of data relative to the swelling degree $Q_e$ for different series of gels (Tables 2–4). For $\alpha/\kappa$ values larger than 1, the data are fitted satisfactorily in the log–log representation by straight lines with slopes close to the theoretical prediction 1.2 (eq 18). This agreement is found as well for the gels neutralized prior to synthesis as for gels neutralized afterward. Deviations from the power law behavior can be observed for $\alpha/\kappa$ values smaller than 1 and correspond in fact to deswollen gels with concentrations larger than in the reaction bath. One notices that the data relative to the smallest ionization degree ($f = 0.1$) are shifted upward in this representation. This might be due to small changes in the prefactor of the osmotic pressure (eq 6), which depends on the ionization degree. It can be noted that data from Figure 17a–c do collapse on a single curve when plotted on the same graph. However, this feature is only fortuitous and results from a compensation between varying cross-linking degree and concentration in the reaction bath to obtain about the same value for the polymerization degree $N$ of the effective elastic strands. That parameter enters into eq 18 and plays a role as demonstrated by the fact that data from Figure 17d do not superimpose on those from Figure 17a–c.

The variation of the equilibrium shear modulus $\mu_e$ with the parameter $\alpha/\kappa$ is depicted in Figure 18. Two regimes are observed: at low $\alpha/\kappa$ values, i.e. for small swelling ratios, $\mu_e$ decreases with $\alpha/\kappa$ until a minimum and then, for the larger swelling ratios, $\mu_e$ increases. In the whole range, the variations relative to the different ionization degrees cannot be superimposed satisfactorily as a function of $\alpha/\kappa$. Again the prefactor in the osmotic pressure might be responsible for that effect. At low $\alpha/\kappa$, the shear modulus decrease can be approximated by power laws with exponents ranging between −1/2 and −1.

The parameter $\alpha/\kappa$ can be eliminated between eqs 18 and 22, which amounts to eliminating the excluded volume parameter in these expressions. The resulting

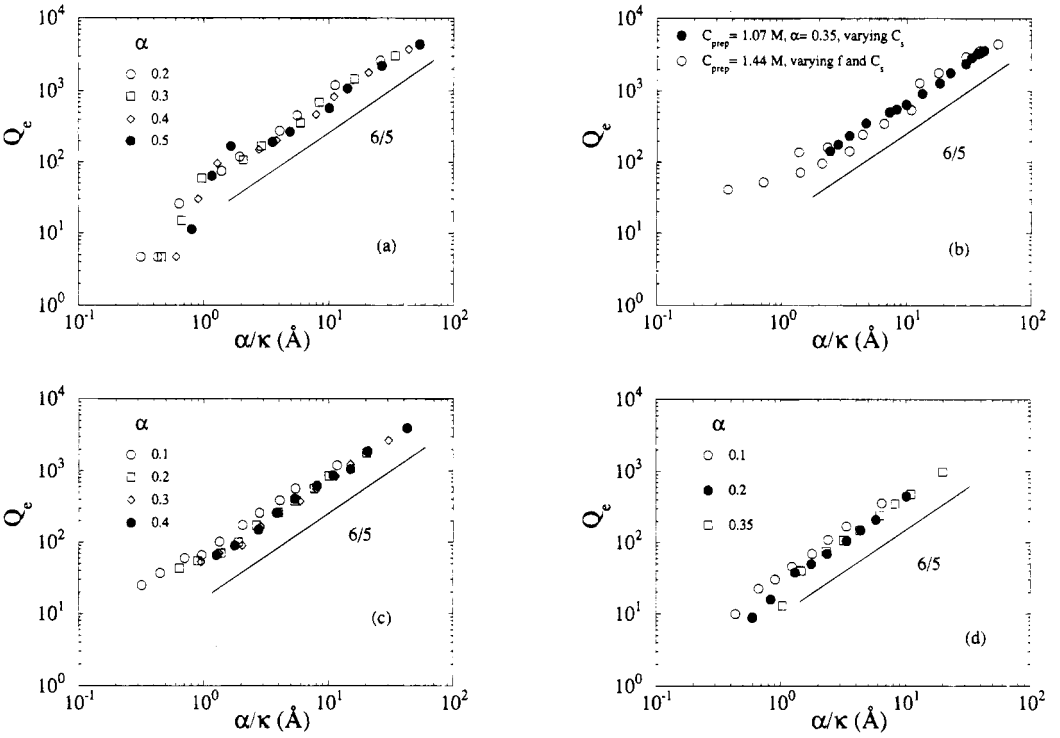


**Figure 17.** Variation of the swelling ratio $Q_e$ as a function of $\alpha/\kappa$ for gels with different conditions of preparation: (a) $C_{prep} = 1.44$ M, $r_c = 0.5\%$, ionized after the gelation; (b) $C_{prep}$ as indicated, $r_c = 0.47\%$, ionized before the gelation (data from ref 30); (c) $C_{prep} = 1.11$ M, $r_c = 1\%$, ionized after the gelation; (d) $C_{prep} = 1.11$ M, $r_c = 2\%$, ionized after the gelation. The straight lines show the predicted 6/5 slope (eq 18).

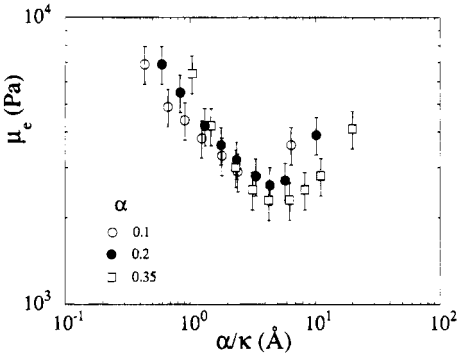


**Figure 18.** Shear modulus as a function of $\alpha/\kappa$ for gels at swelling equilibrium. The latter is varied by changing the salt concentration, and the cross-linking ratio is constant, $r_c = 0.02$ (data from Table 2).

equation

$$\mu_e \sim k_B T N^{-4/3} a^{-3} Q_e^{-1/3} \tag{29}$$

expresses simply the affine character of the deformation, which was assumed in the model. The experimental variation of $\mu_e$ as a function of $Q_e$ is given in Figure 19. Within experimental accuracy, the data are consistent with the affine deformation assumption in the range where $\mu_e$ decreases with increasing swelling ratio $Q_e$. Exponents of the power law $\mu_e(Q)$ between 1/3 and 0.6 have been reported for a number of osmotic deswelling experiments in good solvent conditions.[23,40-42] Values of the exponent larger than 1/3 were attributed to a consequence of a deinterpenetration process.[23] Also, in the same conditions, the model proposed by Panyukov[10] and Obukhov et al.[11] predicts an exponent of 7/12 for gels in good solvents. It must, however, be remarked that these results refer to deswelling experiments in which the excluded volume parameter remains constant, the gels being immersed in concentrated solutions of long chains. Our study concerned gels at the swelling equilibrium, the excluded volume parameter being varied by addition of salt and/or change of ionization degree. For a neutral gel, the $C^*$ theorem, based on the packing condition,[9] predicts that, under a variation of the excluded volume parameter resulting from an interchange of solvent, the shear modulus $\mu_e \sim k_B T/R_e^3$ is inversely proportional to $Q_e$. In the case of ionized gels, even the smallest swelling ratios are already of the same order of magnitude as the equilibrium swelling ratios in neutral gels. Therefore it can be expected that higher swelling ratios at smaller salt concentrations can be obtained only by stretching the polymer chains.

At this point it is interesting to refer back to the Panyukov and Obukhov et al. approach[10,11] and to examine the experimental data in the light of their model. It is still assumed that swelling causes junctions to move affinely; that is, they move apart by the same linear expansion $\lambda$ as the macroscopic network, $\lambda = (Q_e/Q_0)^{1/3}$, with $Q_0$ being the swelling ratio in the preparation state. The end-to-end distance $R_e$ becomes $\lambda R_{prep}$ under swelling, $R_{prep}$ being the same quantity in the preparation state, but the end-to-end distance in the reference state is now taken to be that of a free chain in a solution at concentration $\phi_e$. The scaling result is used for the osmotic pressure, i.e., $\Pi_{os}/k_B T \sim \xi^{-3}$, where $\xi$ is the correlation length, and no packing assumption is used. In the case of gels prepared in the absence of charges ($\Theta$ solvent) and then ionized and swollen at equilibrium in the presence of a salt excess, $R_{prep}$ corresponds to Gaussian strands and the end-to-end distance in the reference state is given by eq 24. It follows that

$$\begin{aligned} Q_e &\sim N^{3/5} a^{-9/5} Q_0^{2/5} v_e^{3/5} \\ \mu_e &\sim k_B T N^{-24/17} a^{-12/17} Q_0^{-9/10} v_e^{-3/5} \\ \mu_e &\sim k_B T a^{-3} N^{-3/4} Q_0^{-1/2} Q_e^{-1} \end{aligned} \tag{30}$$

where the last equation is obtained by eliminating $v_e$

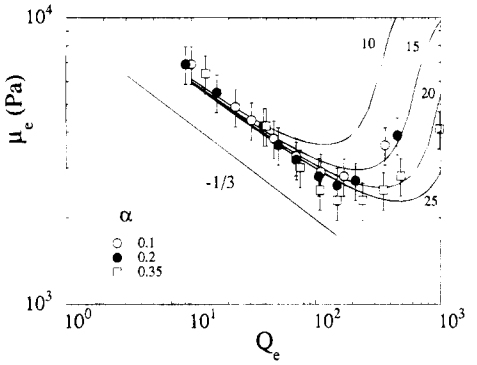


**Figure 19.** Shear modulus as a function of swelling equilibrium ratio (same data as in Figure 18). Continuous lines correspond to predictions from the model based on deviations from Gaussian elasticity at high $Q_e$ values[8] (numbers of statistical units as indicated). An arbitrary normalization was applied to match the calculated curves to the experimental data.

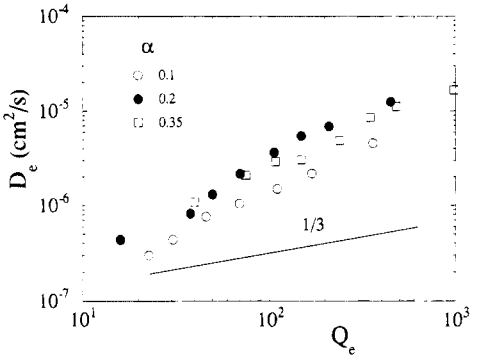


**Figure 20.** Variation of the cooperative diffusion coefficient with equilibrium swelling ratio (data from Table 2). The straight line has the predicted slope in eq 31.

between the two first equations. Taking into account eq 16, the $Q_e$ dependence on $\alpha/\kappa$ is the same as in (18) and in agreement with the data. On the other hand, the $Q_e^{-1}$ dependence for $\mu_e$ does not agree with the experimental behavior in Figure 19. It can also be noted that the use of the scaling result for the osmotic pressure is fully inconsistent with eq 21, which is supported by most experimental results.[12-14,25] However, the use of eq 21 in the model does not provide any better agreement with the experiments since then even the $\alpha/\kappa$ dependence for $Q_e$ is incorrect, with an exponent 30/17, much larger than 6/5.

A related remark is that both the elastic term (eq 5) with the affine deformation hypothesis and the osmotic term (eqs 16 and 21) seem to be correctly estimated in the model by Barrat et al. Thus the right prediction for the $\alpha/\kappa$ dependence of $Q_e$ would not result from the cancellation of two errors as is often the case in Flory type theories.[26] In this context, the shear modulus results in Figure 18 appear even more surprising.

In the high-$Q_e$ range the upturn in $\mu_e$ has already been reported for gels of acrylamide–sodium acrylate copolymers[30] and hydrolyzed polyacrylamide.[8] The results were interpreted as the onset of non-Gaussian elasticity of the chains due to their highly stretched conformation.[39] The strain–stress relation becomes then nonlinear but the shear modulus can still be obtained from the initial slope of the true stress variation versus the deformation function $(\lambda^2 - \lambda^{-1})$. In Figure 19 are reported the curves $\mu_e(Q_e)$ calculated by means of the approach of ref 8 for different values of the number of statistical units between two consecutive cross-links. The agreement is poor but the general behavior of the calculated curves would favor a number of statistical units $N$ about 15–20, which corresponds to a number of monomers $\nu_c$ about 60, significantly larger than estimated in the approximation of an ideal gel. This means that there are many cross-links in efficient in the gel either because of the presence of dangling chains or because they are grouped in small aggregates.

It is also interesting to remark that the upturn of the equilibrium shear modulus occurs for values of $Q_e$ corresponding to a concentration of counterions approximately equal to the salt concentration. At this stage, the chains start to be stretched. In that range, one observes experimentally a nonlinear behavior of the stress versus $(\lambda^2 - \lambda^{-1})$. The observation of a non-Gaussian elasticity in the high-swelling range leads us to question the validity of the derivation of the equilibrium swelling degree. In fact, the upturn of $\mu_e$ in the high-swelling range should lead to a smaller variation of $Q_e$ with $\alpha/\kappa$ in the same range. This is not seen in Figure 17. However, in the representation of Figure 16, there is a partial compensation, as a downwards shift of $Q_e$ is accompanied by a shift to the left of the parameter $\alpha/\kappa$.

Turning now to the dynamical properties, one can express the equilibrium diffusion coefficient as a function of $Q_e$ for gels with constant $N$ by combining eqs 18 and 23. This leads to

$$D_e \sim \frac{k_B T}{\eta_0} N^{-2/3} a^{-1} Q_e^{1/3} \tag{31}$$

The variation of $D_e$ with $Q_e$ is plotted in Figure 20. The diffusion coefficient is found to increase with $Q_e$ as predicted by the theory. It must be noted that the opposite behavior is found for neutral gels.[27] However, one observes a much larger variation of $D_e$ than expected, with an exponent close to 1. Furthermore, the data relative to the lowest ionization degree ($\alpha = 0.1$) are shifted to lower values.

One can note that eq 31 is based on eq 23, which has been derived from eq 14, assuming a monotonous variation for $\mu_e$ as a function of $\alpha/\kappa$ (eq 22). The latter is not obeyed for large $Q_e$ values. Therefore it is interesting to combine directly the experimental results according to eq 14, which is more general than eq 31 and does not rely on the $\alpha/\kappa$ dependence of the experimental quantities. Combining (9) and (14), one gets

$$D_e \sim \frac{a^2 N^{2/3}}{\eta_0} \mu_e Q_e^{2/3} \tag{32}$$

Figure 21 shows the log–log variation of the ratio $D_e/\mu_e$ as a function of $Q_e$ for the series of gels whose characteristics are given in Table 2. Again one observes the small shift between the samples with $\alpha = 0.1$ and those with higher ionization degree. Even if the data analysis is restricted to the lowest $Q_e$ range, a search for a power law behavior would yield exponents about 1, larger than the predicted 2/3 value. Thus, even the validity of eq 14 seems to be questioned.

A possible explanation lies in the complexity of the medium that contains three different components: monomers, counterions ($Na^+$), and salt ions ($Na^+$ and $Cl^-$), the small amount of $H^+$ ions resulting from the spontaneous dissociation of the monomers being neglected. This implies three eigenvalues for the matrix of the

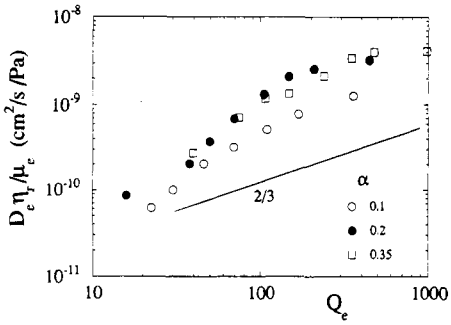


**Figure 21.** Plot of the ratio $\eta_r D_e/\mu_e$ as a function of $Q_e$ (eq 32), $\eta_r$ being the ratio of solvent viscosity to pure water viscosity. The straight lines shows the prediction from eq 32.

relaxation rates of concentration fluctuations and thus three characteristic decay rates, which have been discussed in detail by Ajdari et al.[13,43,44] The fastest mode is the plasmon mode, which corresponds to the restoration of electroneutrality through fast nondiffusive motion of the small ions. The two remaining modes are diffusive and must participate in the kinetics of swelling. The fastest mode corresponds to the time scales where the Donnan equilibrium is restored and is characterized by a diffusion coefficient $D_{\text{Donnan}}$, typically $10^{-5}$ cm$^2$ s$^{-1}$. The slowest relaxation mode is the one we have considered up to now and is related to the collective motion of polymer chains with electroneutrality and Donnan equilibrium being preserved.[43] In fact, it can be seen in Figure 16 that the experimental values of $D_e$ in the high-swelling limit are of the same order of magnitude as the diffusion coefficients of ions. Both swelling and Donnan equilibration proceed with about the same rate. Therefore the assumption that the Donnan and collective motion modes are uncoupled is likely to be nonvalid. One must also note that this coupling effect between the two modes must affect the determination of $\mu_e/M_{os}$ from the kinetics of swelling experiments.

## Conclusion

The results reported in this paper illustrate the effect of electric charges on the thermodynamic properties of gels. Moderately cross-linked gels of PAA prepared at low pH and subsequently ionized have been studied by means of different techniques: static and dynamic light scattering, kinetics of swelling, and uniaxial compression experiments.

At a fixed polymer concentration, close to that of preparation, the shear modulus is found to decrease upon increasing the ionization degree. This result can be explained by assuming that the reference state used to compute the elastic part of the free energy is changed upon ionization of the chains.[10,11] However, that assumption fails to explain swelling equilibrium results. An alternate explanation takes into account the tendency of these systems to undergo microscopic phase segregation. That behavior is observed as well for PAA solutions but is coupled in the case of gels to the frozen inhomogeneities associated with the formation of the network, i.e., the radical copolymerization of cross-links and monomers with different reactivities. We believe that the elastic properties of the gels reflect complicated averages between the elastic contributions from dense and more dilute regions and that the respective weights of these contributions can be modified upon ionization and partial rearrangement of the chains, as long as the cross-linking degree is not too high. While this picture is only conjectural and qualitative, it is supported by light scattering results that show a decrease of the frozen-in component upon ionization. Would this conjecture be correct, then this would be the first experimental evidence of a correlation between the macroscopic properties and the submicroscopic structure.

The properties of gels swollen at equilibrium in solvents with different salt contents can be described by a simple picture of gels swollen by an electrostatic excluded volume proportional to $(\alpha/\kappa)^2$. Surprisingly, the excluded volume approach in the strong screening regime and the Donnan equilibrium model in the weak screening regime lead to the same prediction for the equilibrium swelling degree. This is probably not merely coincidental and might have some physical meaning. In fact, most of the results have been obtained in the strong screening regime. It appears that for gels formed from flexible chains the weak screening regime seems to be unattainable at any cross-link density as shown by the following observation: according to eqs 8 and 9 relative to salt-free gels $R_e \sim a^{-1/2}\phi_e^{-1/2}\alpha^{-1/4}$ whereas $\kappa \sim (4\pi l_B)^{1/2}\phi_e^{1/2}\alpha^{1/2}$, so that $\kappa R_e \sim \alpha^{1/4}$ is independent of $N$ and $\phi_e$ and can be decreased only by a reduction of $\alpha$, in which case other effects associated with backbone interactions come into play.

The swelling equilibrium degree was found to scale like $(\alpha/\kappa)^{6/5}$ whatever the conditions of synthesis for the gels. For given cross-linking degree and concentration of preparation, the plots of $Q_e$ vs $\alpha/\kappa$ lead to a good superposition of the data except for the smallest ionization degree ($f = 0.1$), maybe due to a prefactor effect in the expression for the osmotic pressure. The 6/5 slope is always obeyed, in agreement with the model.[9]

On the other hand, the shear modulus results are not well described by the model and the $(\alpha/\kappa)^{-2/5}$ dependence is not clearly observed. However, as long as the equilibrium swelling degree is not too large, they are consistent with the postulated affine deformation process, which might be favored by a better homogeneity of the gels, due to the presence of electrical charges, and by the large swelling degrees that facilitate the deinterpenetration of the chains. In the limit of very high swelling degree, where the chains become strongly stretched, the shear modulus is no longer given by Gaussian elasticity and increases with the swelling ratio.

Finally, measurements of the kinetics of swelling allow one to determine an effective diffusion coefficient of the gels at the swelling equilibrium. This coefficient is found to increase with the swelling degree, contrary to what is observed for neutral gels and in qualitative agreement with the predictions of an approach based on an electrostatic excluded volume. However, the variation of the diffusion coefficient with $\alpha/\kappa$ or with the swelling degree is much larger than predicted. This could be partly due to the coupling between the establishment of a Donnan equilibrium and the collective diffusion of the network strands, coupling that is not taken into account by the model.

Several concluding remarks can be made. In neutral gels it was found that topological defects, such as dangling ends in the network, affect the shear modulus sooner than the equilibrium swelling degree.[45] Thus it would be tempting to consider that the data reported here support the picture by Barrat et al., at least as far as only static equilibrium properties are concerned, the departure of shear modulus results from the prediction being attributed to the complex structure of these gels.

However, it must recognized that such a simple picture makes no room for the variation of persistence length with neutralization and salt content, a problem still under debate today.[38,46] In this context, the success of eq 18 in describing the equilibrium ratio of our gels might be only fortuitous. Anyway this equation provided a very useful hint for a new powerful representation of these data. A theoretical justification for this phenomenological equation may still need to be found.

**Acknowledgment.** We are grateful to J. F. Joanny and P. Pincus for continuous interactions during this work. Helpful discussions with M. Rubinstein are also gratefully acknowledged.

## References and Notes

(1) Katchalsky, A.; Lifson, S.; Heisenberg, H. *J. Polym. Sci.* **1951**, *7*, 571.
(2) Katchalsky, A.; Michaeli, J. *J. Polym. Sci.* **1955**, *9*, 69.
(3) Flory, P. J. *The Principles of Polymer Chemistry*; Cornell University Press: Ithaca, NY, 1953.
(4) Hasa, J.; Ilavsky, M.; Dusek, K. *J. Polym. Sci.* **1975**, *13*, 253.
(5) Ricka, J.; Tanaka, T. *Macromolecules* **1984**, *17*, 2916.
(6) Brannon-Peppas, L.; Peppas, N. A. *Polym. Bull.* **1988**, *20*, 285.
(7) Konak, C.; Bansil, R. *Polymer* **1989**, *30*, 677.
(8) Schröder, U. P.; Oppermann, W. *Makromol. Chem., Macromol. Symp.* **1993**, *73*, 63.
(9) Barrat, J. L.; Joanny, J. F.; Pincus, P. *J. Phys. II Fr.* **1992**, *2*, 1531.
(10) Panyukov, S. V. *Sov. Phys.—JETP (Engl. Transl.)* **1990**, *71*, 372.
(11) Obukhov, S. P.; Rubinstein, M.; Colby, R. H., preprint.
(12) Schosseler, F.; Ilmain, F.; Candau, S. J. *Macromolecules* **1991**, *24*, 225.
(13) Schosseler, F.; Moussaid, A.; Munch, J. P.; Candau, S. J. *J. Phys. II Fr.* **1991**, *1*, 1197.
(14) Moussaid, A.; Munch, J. P.; Schosseler, F.; Candau, S. J. *J. Phys. II Fr.* **1991**, *1*, 637.
(15) Skouri, R.; Munch, J. P.; Schosseler, F.; Candau, S. J. *Europhys. Lett.* **1993**, *23*, 635.
(16) Joosten, J. G. H.; McCarthy, J. L.; Pusey, P. N. *Macromolecules* **1991**, *24*, 6690.
(17) Pusey, P. N.; Van Megen, W. *Physica A* **1989**, *157*, 705.
(18) Moussaid, A.; Candau, S. J.; Joosten, J. G. H. *Macromolecules* **1994**, *27*, 2102.
(19) Li, Y.; Tanaka, T. *J. Chem. Phys.* **1990**, *92*, 1365.
(20) Peters, A.; Hocquart, R.; Candau, S. J. *Polym. Adv. Technol.* **1992**, *2*, 285.
(21) James, H.; Guth, E. *J. Polym. Sci.* **1949**, *4*, 153.
(22) See, for instance: Dusek, K.; Prins, W. *Adv. Polym. Sci.* **1969**, *6*, 1.
(23) Bastide, J.; Candau, S. J.; Leibler, L. *Macromolecules* **1980**, *14*, 719.
(24) Joanny, J. F.; Pincus, P. *Polymer* **1980**, *21*, 274.
(25) Weill, C.; Lachhab, T.; Moucheront, P. *J. Phys. II Fr.* **1993**, *3*, 927.
(26) de Gennes, P. G. *Scaling Concepts in Polymer Physics*; Cornell University Press: Ithaca, NY, 1979.
(27) Munch, J. P.; Candau, S. J.; Herz, J.; Hild, G. *J. Phys. (Paris)* **1977**, *38*, 971.
(28) Candau, S. J.; Bastide, J.; Delsanti, M. *Adv. Polym. Sci.* **1982**, *44*, 27.
(29) Yamaguchi, M.; Wakutsu, M.; Takahashi, Y.; Noda, I. *Macromolecules* **1992**, *25*, 470.
(30) Ilmain, F. Thesis, Strasbourg, 1991.
(31) Schosseler, F.; Skouri, R.; Munch, J. P.; Candau, S. J. *J. Phys. II Fr.* **1994**, *4*, 1221.
(32) Candau, S. J.; Young, C.; Tanaka, T.; Lemaréchal, P.; Bastide, J. *J. Chem. Phys.* **1979**, *70*, 4694.
(33) Geissler, E.; Hecht, A. M. *J. Phys. Lett. (Paris)* **1979**, *40*, L173.
(34) Geissler, E.; Horkay, F.; Hecht, A. M. *Phys. Rev. Lett.* **1993**, *71*, 645.
(35) Xue, J. Z.; Pine, D. J.; Milner, S. T.; Wu, X. L.; Chaikin, P. M. *Phys. Rev. A* **1991**, *46*, 6550.
(36) Borue, V.; Erukhimovich, I. *Macromolecules* **1988**, *21*, 3240.
(37) Joanny, J. F.; Leibler, L. *J. Phys. (Paris)* **1990**, *51*, 545.
(38) Barrat, J. L.; Joanny, J. F. *Europhys. Lett.* **1993**, *24*, 333.
(39) Treloar, L. R. G. *The Physics of Rubber Elasticity*; Clarendon Press: Oxford, 1975.
(40) Horkay, F.; Hecht, A. M.; Geissler, E. *J. Chem. Phys.* **1989**, *91*, 2706; *Macromolecules* **1989**, *22*, 2007.
(41) Horkay, F.; Burchard, W.; Hecht, A. M.; Geissler, E. *Macromolecules* **1993**, *26*, 4203.
(42) Ilavsky, M.; Bouchal, K.; Dusek, K. *Makromol. Chem.* **1989**, *190*, 883.
(43) Ajdari, A.; Leibler, L.; Joanny, J. F. *J. Chem. Phys.* **1991**, *95*, 4580.
(44) Moussaid, A.; Schosseler, F.; Munch, J. P.; Candau, S. J. *Macro-ion Characterization: From Dilute Solutions to Complex Fluids*; Schmitz, K. S., Ed.; ACS Symposium Series 548; American Chemical Society: Washington, DC, Chapter 22.
(45) Bastide, J.; Picot, C.; Candau, S. J. *J. Polym. Sci.* **1979**, *17*, 1441.
(46) Degiorgio, V.; Mantegazza, F.; Piazza, R. *Europhys. Lett.* **1991**, *15*, 75.